Published in final edited form as:

Langmuir. 2019 November 19; 35(46): 14939–14948. doi:10.1021/acs.langmuir.9b02971.

Strategy to Identify Improved *N*-Terminal Modifications for Supramolecular Phenylalanine-Derived Hydrogelators

Brittany L. Abraham, **Wathsala Liyanage**, **Bradley L. Nilsson**

Department of Chemistry, University of Rochester, Rochester, NY 14627-0216, USA.

Abstract

Supramolecular hydrogels formed by self-assembly of low molecular weight (LMW) compounds have been identified as promising materials for applications in tissue engineering and regenerative medicine. In many cases, the relationship between the chemical structure of the gelator and the emergent hydrogel properties is poorly understood. As a result, empirical screening strategies instead of rational design approaches are often relied upon to tune the emergent properties of the gels. Herein, we describe a novel strategy to identify improved phenylalanine (Phe) derived gelators using a focused empirical approach. Fluorenylmethoxycarbonyl (Fmoc) protected Phe derivatives are a privileged class of gelators that spontaneously self-assemble into fibrils that entangle to form a hydrogel network upon dissolution into water. However, the Fmoc group has been shown to have toxicity drawbacks for potential biological applications, requiring the identification of new *N*-terminal modifications that promote efficient self-assembly but lack the shortcomings of the Fmoc group. We previously discovered that fibrils in Fmoc-*p*-nitrophenylalanine (Fmoc-4-NO_2-Phe) hydrogels transition to crystalline microtubes after several hours by a mechanism that involves the hierarchical assembly and fusion of the hydrogel fibrils. We hypothesized that this hierarchical crystallization behavior could form the basis of a screening approach to identify alternative *N*-terminal functional groups to replace Fmoc in Phe-derived LMW gelators. Specifically, screening *N*-terminal modifying groups for 4-NO_2-Phe that stabilize the hydrogel state by preventing subsequent hierarchical crystallization would facilitate empirical identification of functional Fmoc replacements. To test this approach, we screened a small series of 4-NO_2-Phe derivatives with various *N*-terminal modifying groups to determine if any provided stable LMW supramolecular hydrogels. All but one of the 4-NO_2-Phe derivatives assembled into crystalline forms. Only the 1-naphthaleneacetic acid (1-Nap) 4-NO_2-Phe derivative self-assembled into a stable hydrogel network. Additional Phe derivatives were modified by *N*-terminal 1-Nap-Phe groups to confirm the general potential of 1-Nap as a suitable replacement for Fmoc, and all derivatives formed stable hydrogels under similar conditions to their Fmoc-Phe counterparts. These results illustrate the potential of this approach to identify next-generation Phe-derived LMW gelators with improved emergent properties.

Graphical Abstract

bradley.nilsson@rochester.edu, Fax: +1 585 276-0205; Tel. +1 585 276-3053.

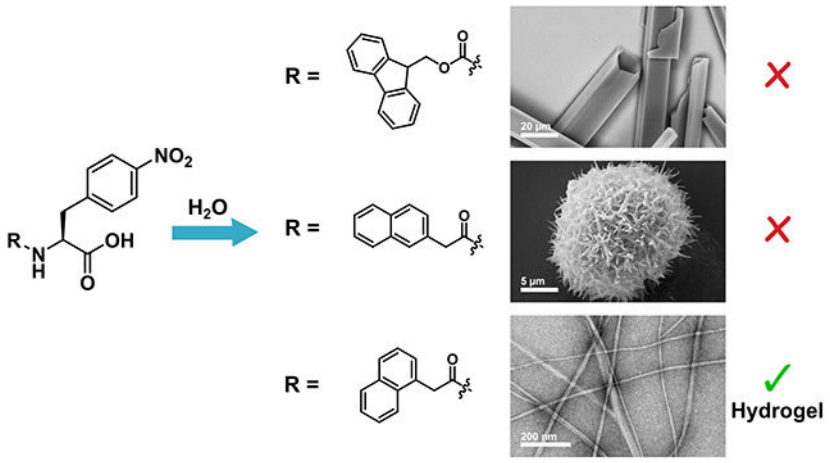

Keywords

Experimental synthetic protocols; compound characterization data; additional digital images; rheological data

Introduction

Supramolecular hydrogels are attracting increasing interest as biomaterials for applications in tissue engineering and regenerative medicine.[1–7] Polymer-based materials have been widely studied for such applications,[8–9] but hydrogels formed from self-assembling biomolecules are emerging as next-generation biomaterials due to advantages in emergent properties.[10–14] Peptide-based hydrogels have garnered special interest due to their biocompatibility, shear-responsive performance, and tunable emergent properties via sequence modification.[15–20] The impressive potential of self-assembling peptide hydrogels for tissue engineering *in vitro* and *in vivo* has been illustrated in several landmark studies,[21–22] but a major impediment to the widespread adoption of these materials is the high cost of peptide production.[4,18] As a result, low molecular weight (LMW) supramolecular gelators have been investigated as cost-effective alternatives to peptides.[23–26] Supramolecular hydrogels derived from inexpensive LMW compounds that are biocompatible, optically transparent, shear-responsive, and that form rapidly in physiologically relevant conditions would be transformative next-generation biomaterials for tissue engineering.[27–28] Unfortunately, most hydrogels derived from LMW gelators are often deficient in one or more of these properties.[28] The current lack of understanding of how the molecular structure of supramolecular LMW gelators correlates with the emergent hydrogel properties has complicated the development of materials with all the requisite properties for biological applications.[29]

Modified phenylalanine (Phe) derivatives are privileged LMW supramolecular gelators that self-assemble through noncovalent interactions to form fibrils which subsequently entangle to trap water and form a hydrogel network.[30–34] Phe-derived hydrogels have potential use as antibacterial agents, as drug delivery agents, and as scaffolds for tissue engineering.[35–45] The most ubiquitous modification of Phe to promote self-assembly and gelation is the *N*-

terminal fluorenylmethyloxycarbonyl (Fmoc) group.[46–49] Fmoc plays a critical role in promoting self-assembly through aromatic π-π stacking interactions between neighboring fluorenyl moieties in self-assembled structures.[32,50–51] The well-studied dipeptide Fmoc-diphenylalanine (Fmoc-FF) forms hydrogels at physiological pH that were shown to be suitable for application in drug delivery and tissue engineering by Gazit and coworkers.[37] Subsequently, Ulijn and coworkers demonstrated *in vitro* three-dimensional tissue culture in hydrogels formed from either Fmoc-FF self-assembly or coassembly with fibronectin-derived Fmoc-Arg-Gly-Asp (Fmoc-RGD), to promote integrin-mediated cell adhesion.[38–40] We have previously shown that Phe-containing dipeptides Fmoc-FR and Fmoc-FD coassemble to form a hydrogel where the RGD motif is mimicked on the supramolecular fibril surface, enabling successful cell adhesion and proliferation on the hydrogel surface.[52] Despite these achievements, incorporation of Fmoc into supramolecular biomaterials is problematic. It has been shown that Fmoc-containing gelators become necrotic to some human cell lines over longer incubation periods due to byproducts of Fmoc degradation.[53] Additionally, the chemical instability of the carbamate linker at higher pH can also cause partial Fmoc deprotection during the gelation process if performed via pH switching.[54–55] Herein, we report a focused empirical approach that enables identification of suitable alternatives to Fmoc for *N*-terminal modification of Phe derivatives to provide hydrogels with robust emergent properties.

We devised an empirical screening strategy based on competing self-assembly processes leading to emergent hydrogel or crystal states to identify non-Fmoc *N*-terminal modifications that promote functional gelation. The relationship between hydrogelation and crystallization self-assembly pathways is poorly understood, but it has been theorized that three-dimensional crystals represent a stable thermodynamic state of assembly while unidirectional fibrils or worm-like micelles observed in hydrogel networks represent a kinetically trapped state.[56–57] We previously reported that the gelator Fmoc-*p*-nitrophenylalanine (Fmoc-4-NO_2-Phe, **1**) spontaneously crystallizes from the hydrogel state after several hours (Figure 1).[58] This crystallization proceeds by a hierarchical process in which initially formed fibrils further align and assemble into crystals over time.[59] Similar behavior has been reported for a handful of other LMW gelators,[56,60–63] but we found that among other Fmoc-Phe derivatives studied previously, this behavior was enhanced in the Fmoc-4-NO_2-Phe derivative.[64–66] We leveraged this tendency for 4-NO_2-Phe derivatives to undergo ultimate crystallization to screen for an *N*-terminal modification (X) that would prevent an X-4-NO_2-Phe derivative from proceeding to the crystalline state, thus stabilizing a hydrogel state. We hypothesized that a modifying group that afforded a stable hydrogel in this screen would be a suitable replacement for Fmoc in other LMW Phe-derived gelators.

Accordingly, we prepared a focused collection of five 4-NO_2-Phe derivatives to screen for stabilization of hydrogel assemblies. The selection of *N*-terminal groups was inspired by literature precedent for peptide and amino acid gelators. Phenylalanine-based gelators with naphthyl groups at the *N*-terminus have been frequently used by Xu *et al.* and Adams *et al.*[43,67] Pyrene is another aromatic moiety that has been conjugated to phenylalanine to promote gelation by Banerjee and coworkers.[68] Lipid chains and other aliphatic groups have also been utilized as a non-aromatic means of inducing gelation of amino acids.[41,69–70] Of

the five *N*-terminal groups screened, only the derivative conjugated with 1-naphthaleneacetic acid (1-Nap), 1-Nap-4-NO_2-Phe, afforded a stable hydrogel. Based on this outcome, we then prepared three other 1-Nap modified derivatives from Phe and Phe derivatives that have been shown to form stable hydrogels with Fmoc-modification.[32,64] All three 1-Nap-Phe derivatives were found to form translucent hydrogels with appropriate viscoelastic properties for potential biological applications like tissue engineering or drug delivery. Thus, this 4-NO_2-Phe-based screening approach successfully identified an *N*-terminal modification that promotes gelation as efficiently as the frequently employed Fmoc group. This strategy can be effectively employed in the empirical identification of next-generation LMW hydrogel biomaterials derived from Phe and its derivatives without the need for initial understanding of structure-function relationships in the proposed gelators.

Materials and Methods

Materials.

Reagents and organic solvents were purchased commercially and used without further purification. Fmoc-amino acids were purchased at the highest available commercial quality and used directly in gelation experiments without further purification. Synthetic details and characterization data for compounds **2–6** and **10–12** are reported in the Supporting Information. Water used for gelation was purified using a nanopure filtration system (Barnstead NANOpure, 0.2 μm filter, 18 Ω).

NMR Spectroscopy.

NMR spectra were recorded using Brüker Avance 400 and 500 MHz spectrometers. ^{1}H, ^{13}C, and ^{19}F chemical shifts are reported as δ with reference to TMS at 0 ppm for ^{1}H, residual solvent for ^{13}C, and $CFCl_3$ at 0 ppm for ^{19}F NMR. See the Supporting Information for NMR spectra and tabulated data.

Self-Assembly and Hydrogelation Conditions.

For self-assembly and hydrogelation triggered by the DMSO solvent switch method, each compound was dissolved in DMSO at a concentration of 247 mM. To trigger self-assembly and hydrogelation, the DMSO stock solution was diluted into water to a final concentration of 4.9 mM (2% DMSO/H_2O, *v/v*) and gently mixed with a mechanical pipettor. Immediately following mixing, an opaque suspension formed that either became a transparent or translucent hydrogel after 1–5 minutes or precipitated from solution depending on the compound used.

For self-assembly and hydrogelation triggered by the glucono-δ-lactone (GdL) pH switch method, each compound was dissolved in water at a concentration of 7.5 mM using one molar equivalent of 0.1 M aqueous NaOH. A fresh aqueous stock solution of GdL was prepared at a concentration of 100 mg/mL (561 mM) immediately prior to gelation experiments. To trigger gelation, 53.4 μL of the GdL stock solution (two molar equivalents) was added to a glass vial containing 2 mL of the 7.5 mM gelator solution and the vial was agitated with a vortex mixer for five seconds. The vials were left undisturbed overnight as the hydrogels formed over the course of several hours.

Transmission Electron Microscopy (TEM).

TEM images were obtained using a Hitachi 7650 transmission electron microscope with an accelerating voltage of 80 kV. Samples of self-assembled materials (10 μL) were applied directly onto 100 mesh carbon-coated copper grids and allowed to stand for 2 minutes. Excess sample was carefully removed by capillary action using filter paper, then the grids were stained with uranyl acetate (8 μL) for 2 minutes. Excess stain was removed via capillary action and the grids were allowed to air dry for 10 minutes. Fibril dimensions were determined using ImageJ software and are reported as the average of at least 100 independent measurements with error reported as the standard deviation about the mean value for these measurements.

Scanning Electron Microscopy (SEM).

SEM images were obtained using a Zeiss Supra 40VP FESEM scanning electron microscope with an accelerating voltage of 10 kV. A suspension of self-assembled material was placed on a glass slide, and excess solvent was carefully removed by capillary action using filter paper. Then, air-dried samples were sputter-coated with gold at 1 Å s^{-1} using a low vacuum sputter coating system (100 mTorr pressure, 15 mA current).

Rheology.

Rheological measurements were obtained using a TA Instruments Discovery HR-2 rheometer. A 20 mm parallel plate geometry was used for the experiments. Hydrogels were formed using 1 mL of solution in 1.5 mL plastic microcentrifuge tubes. Immediately prior to rheological characterization, the plastic tube containing the hydrogel was cut at the 0.5 mL line using a razor blade and the cylindrical hydrogel was placed directly on the rheometer stage for characterization (Figure S19, Supporting Information). Experiments were performed using a 1.2 mm gap size operating in oscillatory mode. Strain sweep experiments were performed from 0.01 to 100 % strain at a frequency of 6.283 rad s^{-1} to determine the linear viscoelastic region for each hydrogel. See the Supporting Information for strain sweep data (Figures S20 and S21). Frequency sweep experiments were performed from 0.1 to 100 rad s^{-1} at constant strain of 1%, which falls within the linear viscoelastic region for each hydrogel. Reported values for storage and loss moduli (G' and G'', respectively) are the average of at least three distinct measurements on separate hydrogels with error reported as the standard deviation about the mean. See the Supporting Information for the three frequency sweeps averaged for each compound (Figures S22 and S23).

Results and Discussion

The Effect of *N*-Terminal Functionalization on Self-Assembly, Hydrogelation, and Crystallization of 4-NO_2-Phe Derivatives.

Five derivatives of *N*-terminally modified 4-NO_2-Phe (**2-6**, Figure 2) were synthesized by coupling 4-NO_2-Phe with the corresponding carboxylic acid derivative of the modifying group via amide bond formation. Detailed synthetic protocols and characterization data may be found in the Supporting Information. Aromatic interactions and the hydrophobic effect have been implicated as important interactions in the self-assembly process, so the

modifying groups screened were either aromatic/hydrophobic, represented by naphthalene and pyrene groups, or aliphatic/hydrophobic, represented by cyclohexyl and hexyl groups. These substituents have been previously used to modify short peptide-based gelators.[43,68–69] The hydrogelation capacity of each derivative was assessed via our previously reported solvent switch conditions.[58] Each compound was dissolved in DMSO to a concentration of 247 mM and subsequently diluted into water to a final concentration of 4.9 mM (2% DMSO/H_2O). Upon dilution into water and gentle mixing, an opaque suspension was formed. Interestingly, the only derivative that formed a stable hydrogel network of one-dimensional fibrils was 1-Nap-4-NO_2-Phe (**3**) (Figure 2E and 2F). Compound **1**, the parent Fmoc-4-NO_2-Phe derivative formed an initial hydrogel that underwent hierarchical assembly into crystalline microtubes as previously reported (Figure 2A and 2B). The remaining derivatives formed either crystalline (compounds **2**, **4**, and **5**; Figure 2C, 2D, and 2G–J) or amorphous (compound **6**, Figure 2K and 2L) precipitates. In the cases of crystalline precipitates, crystal structures were not obtained due to the quality of the crystals obtained from the DMSO solvent switch procedure.

To investigate the nanoscale morphology of crystal states formed by each derivative, SEM or negatively stained TEM images were obtained of each sample 24 hours after initial preparation (Figure 2). Entangled fibrils were only observed in the samples of the 1-naphthalene-modified compound **3** (Figure 2E and 2F), consistent with the macroscopic observation of stable hydrogel formation. Interestingly, compound **2**, which is also a naphthalene based functional group that differs from **3** only in the position of the attachment of the naphthalene group, assembled into microflorettes (Figure 2C and 2D). This is an interesting demonstration of the difficulty in predicting the emergent self-assembly properties of Phe-derived molecules since even subtle structural changes can dramatically modify the assembly characteristics. Compound **1** forms crystalline microtubes as previously reported (Figure 2A and 2B). The aliphatic/hydrophobic cyclohexyl and hexyl modified derivatives **4** and **5** both assembled into crystalline forms, with **4** forming heterogeneous nanocrystals (Figure 2G and 2H) and 5 forming needle-like nanocrystals (Figure 2I and 2J). The assemblies of **5** may not be truly crystalline, but may rather be relatively rigid nanoribbon fibers that are similar to other self-assembled peptide materials. The inability of either of these derivatives to form a hydrogel network is perhaps not surprising due to lack of aromaticity in the *N*-terminal functional group, which has been implicated as a critical feature of Fmoc that encourages self-assembly in LMW gelators.[31,50] Compound **6** formed spherical nanostructures, but no emergent hydrogel properties were observed.

The failure of compounds **1**, **4**, and **6** to assemble into stable hydrogel networks indicates that aromatic character in the *N*-terminal functional group is not alone sufficient to provide structural geometries that facilitate π-π stacking interactions that lead exclusively to assembly into fibril forms. Differences in volume, orientation, and hydrophobicity of the functional group also dictates the ultimate structural fate of molecular assemblies. This is especially underscored when comparing derivatives **2** and **3**, in which the only difference is the position of attachment to the naphthalene ring, yet only **3** forms fibrils capable of supporting a stable hydrogel network. We note that gelators have been previously identified

that incorporate an *N*-terminal pyrene group conjugated to Phe,[68] and a 2-naphthalene group conjugated to Phe or Phe-based dipeptides.[43–44,71–72] However, in the specific case of conjugation of these groups to 4-NO_2-Phe we did not observe hydrogel formation under the conditions used.

Comparison of Self-Assembly and Hydrogelation Properties of Fmoc-X-Phe and 1-Nap-X-Phe Derivatives.

Based on the results of this initial focused screening study, we next sought to confirm that the 1-naphthalene (1-Nap) functional group from compound **3** is a potential functional replacement for Fmoc in other Phe derivatives that have been shown to effectively form hydrogel networks. Three Phe derivatives were chosen for modification with 1-Nap based on the previously reported gelation properties of the corresponding Fmoc-Phe derivatives. Fmoc-Phe (**7**, Figure 3) fails to form hydrogels under solvent switch conditions (dilution from DMSO into water)[32] but does form hydrogels after dissolution in basic water followed by gradual acidification upon hydrolysis of added glucono-δ-lactone (GdL) (pH switch conditions).[54] The fluorinated Fmoc-Phe derivatives Fmoc-3F-Phe (**8**) and Fmoc-F_5-Phe (**9**) (Figure 3) form hydrogels with superior viscoelastic properties to Fmoc-Phe under both solvent switch and pH switch conditions.[32,64] Thus, three derivatives of 1-Nap-X-Phe (**10**-**12**, Figure 3) were synthesized by coupling 1-naphthaleneacetic acid with the corresponding X-Phe amino acid via amide bond formation. Detailed synthetic protocols and characterization data may be found in the Supporting Information. We note that compound **10** has been previously identified as a LMW gelator by Srivastava *et al.*[73]

We first compared self-assembly and gelation of Fmoc and 1-Nap functionalized derivatives using the solvent switch method. Compounds **7**-**12** were dissolved in DMSO as described in the screening studies in the previous section and diluted into water to a final concentration of 4.9 mM (0.5 wt % in 2% DMSO/H_2O, *v/v*). The vials were allowed to stand undisturbed for 3 hours, then they were inverted to assess formation of self-supporting hydrogel networks (see digital images in Figure 4A and 4E). Compound **7** formed an amorphous precipitate under these conditions, while compounds **8** and **9** formed transparent hydrogels stable to vial inversion after several minutes (Figure 4A). Negatively stained TEM images of the precipitate of compound **7** reveals nanoassemblies that vary widely in dimension and morphology and have an average width of 220 ± 77 nm (Figure 4B). TEM images of the hydrogels of compounds **8** and **9** display thin, high aspect ratio fibrils with fibril diameters of 27 ± 3 nm and 16 ± 2 nm, respectively (Figure 4C and 4D). All three 1-Nap modified derivatives formed hydrogels of varying opacity that were stable to vial inversion when prepared by the DMSO dilution method (Figure 4E). Negatively stained TEM images of all three hydrogels showcase the entangled fibril network, with fibril diameters of 95 ± 19 nm, 41 ± 5 nm, and 14 ± 2 nm for compounds **10**, **11**, and **12**, respectively (Figure 4F–4H). A correlation between the opacity of the hydrogel and the fibril diameter was observed for all six compounds, in which thinner fibrils corresponded to a more transparent hydrogel. While not reported herein, structural analysis of how the packing architecture of each derivative dictates the fibril dimensions, and in turn dictates the macroscopic property of hydrogel transparency, is the topic of ongoing study and will be reported in due course.

Hydrogels of 1-Nap-Phe (**10**) and 1-Nap-3F-Phe (**11**) were particularly inhomogeneous due to rapid assembly (Figure 4E). An opaque suspension was observed upon dissolution of the DMSO stock solution into water, which aggregated to form opaque fibrous clumps throughout the resulting hydrogel network if not mixed immediately by pipette. Attempts to mitigate this effect by immediately agitating the vial using a vortex mixer resulted in only fibrous precipitate not stable to vial inversion, likely due to disruption of the rapidly assembling network from the intense agitation. In contrast, when diluting a DMSO stock solution of 1-Nap-F_5-Phe into water, the initial opaque suspension was easily homogenized by gentle mixing before it became transparent after approximately 30 seconds. Thus, slowing the rate of assembly of these materials was deemed necessary to obtain homogeneous, transparent hydrogels required for potential applications in cell culture and tissue engineering.

Optically transparent hydrogels are necessary for biological applications in tissue engineering.[4] To obtain hydrogels with the desired optical transparency, we utilized a method described by Adams and coworkers to form highly homogeneous hydrogels through slow pH adjustment from basic to mildly acidic using glucono-δ-lactone (GdL).[54] Addition of GdL to a high pH aqueous solution of gelator causes slow hydrolysis of GdL, inducing a slow release of protons over the course of several hours that protonate the *C*-terminus of the gelator to trigger self-assembly. While triggering gelation by this pH method lengthens the time required for formation of the hydrogel network, the emergent properties of the hydrogel, including viscoelasticity and optical transparency, are often improved.[54,74] Accordingly, we also assessed gelation of these compounds using the GdL pH switch method to induce self-assembly and gelation. Compounds **7**-**12** were dissolved in water to a concentration of 7.5 mM by adding one equivalent of 0.1 M aqueous NaOH and the resulting solutions were agitated with a mechanical vortex mixer followed by sonication until all gelator was dissolved. Two molar equivalents of GdL were then added from a freshly prepared 100 mg/mL (561 mM) aqueous stock solution to each gelator solution and vials were agitated by vortex mixer for five seconds, then left undisturbed for 24 hours. After 24 hours elapsed, the vials were inverted and digital images were taken (Figure 5A and E). All Fmoc-Phe derivatives formed hydrogels stable to vial inversion under the pH switch conditions used here, but compounds **7** and **8** formed opaque hydrogels whereas compound **9** formed a transparent hydrogel (Figure 5A). Negatively stained TEM images of the opaque hydrogels revealed thicker fibers with varying morphology, with a diameter of 127 ± 48 nm for compound **7** and 126 ± 41 nm for compound **8** (Figure 5B and C). In contrast, thin fibrils with a diameter of 13 ± 2 nm were observed for the transparent hydrogel of compound **9** (Figure 5D). Remarkably, all three 1-Nap-Phe derivatives formed transparent, homogeneous hydrogels stable to vial inversion (Figure 5E). TEM images of the three hydrogels show that they are all comprised of thin, high aspect ratio fibrils with diameters of 11 ± 1 nm, 20 ± 3 nm, and 13 ± 2 nm for compounds **10**, **11**, and **12**, respectively (Figure 5F–H). The superior optical transparency observed in all of the 1-Nap-Phe derived hydrogels compared to their Fmoc counterparts signals that 1-Nap may be a suitable replacement for Fmoc when designing biomaterials for tissue culture applications because transparent hydrogels are necessary to image cells seeded on or embedded within a hydrogel.

The comparative viscoelastic emergent properties of hydrogels of compounds **8**-**12** formed by the GdL pH switch method were investigated using oscillatory rheology (Figure 6A and 6B). Hydrogels were preformed prior to rheological characterization and placed on the instrument stage as a cylindrical hydrogel with an approximate volume of 0.5 mL (Figure S19). Hydrogels of compound **7** were very weak and collapsed during the process of moving the sample from the vial to the rheometer instrument, so no rheological data were collected. Strain sweep measurements were performed on each hydrogel to determine the linear viscoelastic region for each material (Figures S20 and S21). Frequency sweep experiments were then performed for each hydrogel at 1% strain, which was within the linear viscoelastic region for all hydrogels. The viscoelastic parameters measured during each frequency sweep were the storage modulus (G') and the loss modulus (G'') as a function of angular frequency. The storage moduli for the Fmoc-Phe derivatives were nearly independent of frequency, and G' exceeded G'' by an order of magnitude in both cases, indicating a structurally robust material (Figure 6A and Table 1).[75] The observed G' values for the 1-Nap-Phe derivatives were lower than the corresponding Fmoc-Phe derivatives, but in all cases the materials were robust as G' exceeded G'' by an order of magnitude (Figure 6B and Table 1). In the case of compounds **10** and **11**, the storage modulus showed a slight frequency dependence, indicating that a fluid-like behavior is present in the system at high angular frequency, indicating that the network is more dynamic than the corresponding Fmoc-Phe hydrogels.[75]

Collectively, these results indicate that replacement of Fmoc with 1-Nap in Phe-derived gelators produced hydrogels with emergent properties better suited to the demands of certain applications, including *in vitro* cell culture and tissue engineering applications. Using the GdL pH switch method, two of the three Fmoc-Phe derived hydrogels were opaque while all three 1-Nap-Phe derived hydrogels were transparent. Fmoc-Phe and Fmoc-3F-Phe have been shown to form transparent hydrogels using this gelation method under different conditions, but the necessity to use an exact combination of gelator, NaOH, and GdL concentrations to produce a transparent hydrogel makes the Fmoc gelators less versatile as potential biomaterials. The transparency of the Fmoc-F_5-Phe hydrogel seems promising, but this gelator is very hydrophobic due to the pentafluorophenyl side chain, and the hydrogel network precipitates after several days regardless of gelation method used (Figures S24 and S25). Comparatively, the 1-Nap-F_5-Phe hydrogel remains intact for both gelation methods, and only becomes slightly more translucent as time passes (Figures S24 and S25; see Figure S26 for a comparison of the optical transparency of selected Fmoc and 1-Nap derivatives). Hydrogels of 1-Nap-F_5-Phe, as well as the other two 1-Nap-Phe derivatives have been continually stable for two years at room temperature. It is not readily apparent why the change from Fmoc to 1-Nap produces such a dramatic difference, but we are currently initiating interrogation the packing architecture of these systems in order to further understand these changes. The outcome of these structural analyses will be reported in due course.

Forming hydrogels via the pH switch method requires as a first step the dissolution of the gelator at high pH using NaOH. Under these conditions, Fmoc is labile due to the carbamate linkage at the *N*-terminus of the amino acid, and some of the Fmoc can cleave from the Phe

derivative while in this high pH aqueous solution prior to gelation. When Fmoc-Phe derivatives are dissolved in basic solutions, we observed that careful attention must be paid to the precise stoichiometry of NaOH to gelator to avoid the formation of opaque colloidal suspensions; even miniscule excesses of NaOH were found to immediately induce this effect, presumably due to Fmoc lability. This is particularly concerning because degradation of Fmoc-containing hydrogels has been shown to be necrotic to some human cell lines.[53] To address this stability issue, 1-Nap and the other *N*-terminal protecting groups screened in this study were attached to the amino acid via an amide bond. We found that the 1-Nap-Phe derivative, unlike the Fmoc-Phe counterpart, showed no sensitivity to excess NaOH during dissolution of the monomer, consistent with this supposition.

Current efforts in the design of next-generation LMW hydrogels attempt to bridge the gap between empirical and rational design approaches. For example, Adams and coworkers recently reported a computational approach to predict gelation propensity of *N*-terminally protected dipeptides, which identified 9 dipeptide hydrogelators from a library of 2025 dipeptides that were screened *in silico*.[76] A computational approach was also undertaken by Ulijn and coworkers to screen 8,000 tripeptide candidates for self-assembly propensity, leading to the discovery of a four unprotected tripeptide sequences that can form hydrogels at neutral pH.[77] These studies underscore how complex and subtle the correlation between molecular structure and gelation propensity is, where the difference of a single atom can have tremendous effect. Some structural data regarding potential packing architecture for gelators have been obtained using techniques such as cryo-TEM and X-ray diffraction, but significant gaps in understanding in structure activity relationships in the phenomenon of supramolecular gelation persist. Despite these promising new insights that have the potential to advance design of hydrogel materials, empirical approaches and serendipitous discovery still play an important role in this field. Thus, the screening strategy reported herein to identify functional *N*-terminal modifications for supramolecular Phe derived LMW gelators promises to be of great utility for the empirical evaluation of next-generation materials for which completely rational design approaches are not yet possible.

Conclusion

Herein, we have demonstrated an empirical screening approach to identify *N*-terminal functional group modifications that promote efficient self-assembly and hydrogelation of LMW Phe derivatives. This approach leverages the tendency of Fmoc-4-NO_2-Phe fibrils to transition to crystalline microtubes via hierarchical assembly of the initially assembled fibrils. From a focused collection of *N*-terminal functional groups, we identified 1-Nap as the only modified 4-NO_2-Phe derivative that stabilized a unidirectional fibril state that avoided further assembly into crystalline forms, thus providing stable hydrogels. This screening method was further validated by using the identified 1-Nap functional group to modify three other Phe derivatives in order to determine if the capacity for 1-Nap to promote gelation was general to Phe-derived molecules or specific to 4-NO_2-Phe. Efficient gelation was observed on all Phe derivatives that were modified with 1-Nap in this study. In fact, the 1-Nap derivatives demonstrated improved emergent properties relative to the corresponding Fmoc-modified derivatives, including hydrogel stability and optical transparency. Crystallization and hydrogelation are often competing processes in self-assembly and

crystallization often impedes the design of effective LMW agents that promote spontaneous supramolecular gelation. Thus, exploiting a screening method using molecules that have the tendency to crystallize proves to be a stringent test for the identification of functional groups that are highly effective at stabilizing hydrogel states. This novel empirical approach will be of value in the identification of next-generation Phe-derived gelators for which entirely rational design approaches are, as yet, impractical.

Supplementary Material

Refer to Web version on PubMed Central for supplementary material.

Acknowledgements

This work was supported by the National Science Foundation (DMR-1148836) and the National Institutes of Health (National Heart, Lung, and Blood Institute, R01HL138538). BLA was supported by a University of Rochester Sproull Fellowship. We gratefully acknowledge Karen Bentley (URMC Electron Microscope Shared Resource) for her assistance in TEM and SEM imaging experiments.

References

1. Du X; Zhou J; Shi J; Xu B Supramolecular Hydrogelators and Hydrogels: From Soft Matter to Molecular Biomaterials. Chem. Rev. 2015, 115, 13165–13307. [PubMed: 26646318]
2. Webber MJ; Appel EA; Meijer EW; Langer R Supramolecular biomaterials. Nat. Mater. 2015, 15, 13–26.
3. El-Sherbiny IM; Yacoub MH Hydrogel scaffolds for tissue engineering: Progress and challenges. Glob. Cardiol. Sci. Pract. 2013, 2013, 316–342. [PubMed: 24689032]
4. Caliari SR; Burdick JA A practical guide to hydrogels for cell culture. Nat. Methods 2016, 13, 405–414. [PubMed: 27123816]
5. Ye E; Chee PL; Prasad A; Fang X; Owh C; Yeo VJJ; Loh XJ Supramolecular soft biomaterials for biomedical applications. Mater. Today 2014, 17, 194–202.
6. Xu B Gels as Functional Nanomaterials for Biology and Medicine. Langmuir 2009, 25, 8375–8377. [PubMed: 19453130]
7. Hoffman AS Hydrogels for biomedical applications. Adv. Drug Delivery Rev. 2012, 64, 18–23.
8. Sivashanmugam A; Arun Kumar R; Vishnu Priya M; Nair SV; Jayakumar R An overview of injectable polymeric hydrogels for tissue engineering. Eur. Polym. J. 2015, 72, 543–565.
9. Khan F; Tanaka M; Ahmad SR Fabrication of polymeric biomaterials: a strategy for tissue engineering and medical devices. J. Mater. Chem. B 2015, 3, 8224–8249. [PubMed: 32262880]
10. Hosseinkhani H; Hong P-D; Yu D-S Self-Assembled Proteins and Peptides for Regenerative Medicine. Chem. Rev. 2013, 113, 4837–4861. [PubMed: 23547530]
11. Jung JP; Gasiorowski JZ; Collier JH Fibrillar peptide gels in biotechnology and biomedicine. Pept. Sci. 2010, 94, 49–59.
12. Zhao X; Pan F; Xu H; Yaseen M; Shan H; Hauser CAE; Zhang S; Lu JR Molecular self-assembly and applications of designer peptide amphiphiles. Chem. Soc. Rev. 2010, 39, 3480–3498. [PubMed: 20498896]
13. Prince E; Kumacheva E Design and applications of man-made biomimetic fibrillar hydrogels. Nat. Rev. Mater. 2019, 4, 99–115.
14. Dou X-Q; Feng C-L Amino Acids and Peptide-Based Supramolecular Hydrogels for Three-Dimensional Cell Culture. Adv. Mater. 2017, 29, 1604062.
15. Koutsopoulos S Self-assembling peptide nanofiber hydrogels in tissue engineering and regenerative medicine: Progress, design guidelines, and applications. J. Biomed. Mater. Res., Part A 2016, 104, 1002–1016.

16. Rubert Pérez CM; Stephanopoulos N; Sur S; Lee SS; Newcomb C; Stupp SI The Powerful Functions of Peptide-Based Bioactive Matrices for Regenerative Medicine. Ann. Biomed. Eng. 2015, 43, 501–514. [PubMed: 25366903]
17. Guvendiren M; Lu HD; Burdick JA Shear-thinning hydrogels for biomedical applications. Soft Matter 2012, 8, 260–272.
18. Seow WY; Hauser CAE Short to ultrashort peptide hydrogels for biomedical uses. Mater. Today 2014, 17, 381–388.
19. Yu Z; Cai Z; Chen Q; Liu M; Ye L; Ren J; Liao W; Liu S Engineering β-sheet peptide assemblies for biomedical applications. Biomater. Sci. 2016, 4, 365–374. [PubMed: 26700207]
20. Panda JJ; Chauhan VS Short peptide based self-assembled nanostructures: implications in drug delivery and tissue engineering. Polym. Chem. 2014, 5, 4418–4436.
21. Haines-Butterick L; Rajagopal K; Branco M; Salick D; Rughani R; Pilarz M; Lamm MS; Pochan DJ; Schneider JP Controlling hydrogelation kinetics by peptide design for three-dimensional encapsulation and injectable delivery of cells. Proc. Natl. Acad. Sci. U. S. A. 2007, 104, 7791–7796. [PubMed: 17470802]
22. Holmes TC; de Lacalle S; Su X; Liu G; Rich A; Zhang S Extensive neurite outgrowth and active synapse formation on self-assembling peptide scaffolds. Proc. Natl. Acad. Sci. U. S. A. 2000, 97, 6728–6733. [PubMed: 10841570]
23. Johnson EK; Adams DJ; Cameron PJ Peptide based low molecular weight gelators. J. Mater. Chem. 2011, 21, 2024–2027.
24. Fichman G; Gazit E Self-assembly of short peptides to form hydrogels: Design of building blocks, physical properties and technological applications. Acta Biomater. 2014, 10, 1671–1682. [PubMed: 23958781]
25. Ryan DM; Nilsson BL Self-assembled amino acids and dipeptides as noncovalent hydrogels for tissue engineering. Polym. Chem. 2012, 3, 18–33.
26. Draper ER; Adams DJ Low-Molecular-Weight Gels: The State of the Art. Chem 2017, 3, 390–410.
27. Naahidi S; Jafari M; Logan M; Wang Y; Yuan Y; Bae H; Dixon B; Chen P Biocompatibility of hydrogel-based scaffolds for tissue engineering applications. Biotechnol. Adv. 2017, 35, 530–544. [PubMed: 28558979]
28. Vedadghavami A; Minooei F; Mohammadi MH; Khetani S; Rezaei Kolahchi A; Mashayekhan S; Sanati-Nezhad A Manufacturing of hydrogel biomaterials with controlled mechanical properties for tissue engineering applications. Acta Biomater. 2017, 62, 42–63. [PubMed: 28736220]
29. van Esch JH We Can Design Molecular Gelators, But Do We Understand Them? Langmuir 2009, 25, 8392–8394. [PubMed: 19537740]
30. Das T; Haring M; Haldar D; Diaz Diaz D Phenylalanine and derivatives as versatile low-molecular-weight gelators: design, structure and tailored function. Biomater. Sci. 2018, 6, 38–59.
31. Singh V; Snigdha K; Singh C; Sinha N; Thakur AK Understanding the self-assembly of Fmoc–phenylalanine to hydrogel formation. Soft Matter 2015, 11, 5353–5364. [PubMed: 26059479]
32. Ryan DM; Anderson SB; Senguen FT; Youngman RE; Nilsson BL Self-assembly and hydrogelation promoted by F5-phenylalanine. Soft Matter 2010, 6, 475–479.
33. Tamamis P; Adler-Abramovich L; Reches M; Marshall K; Sikorski P; Serpell L; Gazit E; Archontis G Self-Assembly of Phenylalanine Oligopeptides: Insights from Experiments and Simulations. Biophys. J. 2009, 96, 5020–5029. [PubMed: 19527662]
34. German HW; Uyaver S; Hansmann UHE Self-Assembly of Phenylalanine-Based Molecules. J. Phys. Chem. A 2015, 119, 1609–1615. [PubMed: 25347763]
35. Gahane AY; Ranjan P; Singh V; Sharma RK; Sinha N; Sharma M; Chaudhry R; Thakur AK Fmoc-phenylalanine displays antibacterial activity against Gram-positive bacteria in gel and solution phases. Soft Matter 2018, 14, 2234–2244. [PubMed: 29517792]
36. Hu B; Owh C; Chee PL; Leow WR; Liu X; Wu Y-L; Guo P; Loh XJ; Chen X Supramolecular hydrogels for antimicrobial therapy. Chem. Soc. Rev. 2018, 47, 6917–6929. [PubMed: 29697128]
37. Mahler A; Reches M; Rechter M; Cohen S; Gazit E Rigid, Self-Assembled Hydrogel Composed of a Modified Aromatic Dipeptide. Adv. Mater. 2006, 18, 1365–1370.

38. Jayawarna V; Ali M; Jowitt TA; Miller AF; Saiani A; Gough JE; Ulijn RV Nanostructured Hydrogels for Three-Dimensional Cell Culture Through Self-Assembly of Fluorenylmethoxycarbonyl–Dipeptides. Adv. Mater. 2006, 18, 611–614.
39. Jayawarna V; Richardson SM; Hirst AR; Hodson NW; Saiani A; Gough JE; Ulijn RV Introducing chemical functionality in Fmoc-peptide gels for cell culture. Acta Biomater. 2009, 5, 934–943. [PubMed: 19249724]
40. Zhou M; Smith AM; Das AK; Hodson NW; Collins RF; Ulijn RV; Gough JE Self-assembled peptide-based hydrogels as scaffolds for anchorage-dependent cells. Biomaterials 2009, 30, 2523–2530. [PubMed: 19201459]
41. Cao S; Fu X; Wang N; Wang H; Yang Y Release behavior of salicylic acid in supramolecular hydrogels formed by l-phenylalanine derivatives as hydrogelator. Int. J. Pharm. 2008, 357, 95–99. [PubMed: 18329200]
42. Diaferia C; Ghosh M; Sibillano T; Gallo E; Stornaiuolo M; Giannini C; Morelli G; Adler-Abramovich L; Accardo A Fmoc-FF and hexapeptide-based multicomponent hydrogels as scaffold materials. Soft Matter 2019, 15, 487–496. [PubMed: 30601569]
43. Zhang Y; Kuang Y; Gao Y; Xu B Versatile small-molecule motifs for self-assembly in water and the formation of biofunctional supramolecular hydrogels. Langmuir 2011, 27, 529–537. [PubMed: 20608718]
44. Yang Z; Liang G; Ma M; Abbah AS; Lu WW; Xu B d-Glucosamine-based supramolecular hydrogels to improve wound healing. Chem. Commun. 2007, 843–845.
45. Gavel PK; Dev D; Parmar HS; Bhasin S; Das AK Investigations of Peptide-Based Biocompatible Injectable Shape-Memory Hydrogels: Differential Biological Effects on Bacterial and Human Blood Cells. ACS Appl. Mater. Interfaces 2018, 10, 10729–10740. [PubMed: 29537812]
46. Tao K; Levin A; Adler-Abramovich L; Gazit E Fmoc-modified amino acids and short peptides: simple bio-inspired building blocks for the fabrication of functional materials. Chem. Soc. Rev. 2016, 45, 3935–3953. [PubMed: 27115033]
47. Draper ER; Morris KL; Little MA; Raeburn J; Colquhoun C; Cross ER; McDonald TO; Serpell LC; Adams DJ Hydrogels formed from Fmoc amino acids. CrystEngComm 2015, 17, 8047–8057.
48. Adams DJ; Mullen LM; Berta M; Chen L; Frith WJ Relationship between molecular structure, gelation behaviour and gel properties of Fmoc-dipeptides. Soft Matter 2010, 6, 1971–1980.
49. Orbach R; Adler-Abramovich L; Zigerson S; Mironi-Harpaz I; Seliktar D; Gazit E Self-Assembled Fmoc-Peptides as a Platform for the Formation of Nanostructures and Hydrogels. Biomacromolecules 2009, 10, 2646–2651. [PubMed: 19705843]
50. Fleming S; Debnath S; Frederix PWJM; Tuttle T; Ulijn RV Aromatic peptide amphiphiles: significance of the Fmoc moiety. Chem. Commun. 2013, 49, 10587–10589.
51. Orbach R; Mironi-Harpaz I; Adler-Abramovich L; Mossou E; Mitchell EP; Forsyth VT; Gazit E; Seliktar D The Rheological and Structural Properties of Fmoc-Peptide-Based Hydrogels: The Effect of Aromatic Molecular Architecture on Self-Assembly and Physical Characteristics. Langmuir 2012, 28, 2015–2022. [PubMed: 22220968]
52. Liyanage W; Vats K; Rajbhandary A; Benoit DSW; Nilsson BL Multicomponent dipeptide hydrogels as extracellular matrix-mimetic scaffolds for cell culture applications. Chem. Commun. 2015, 51, 11260–11263.
53. Truong WT; Su Y; Gloria D; Braet F; Thordarson P Dissolution and degradation of Fmoc-diphenylalanine self-assembled gels results in necrosis at high concentrations in vitro. Biomater. Sci. 2015, 3, 298–307. [PubMed: 26218120]
54. Adams DJ; Butler MF; Frith WJ; Kirkland M; Mullen L; Sanderson P A new method for maintaining homogeneity during liquid–hydrogel transitions using low molecular weight hydrogelators. Soft Matter 2009, 5, 1856–1862.
55. Sutton S; Campbell NL; Cooper AI; Kirkland M; Frith WJ; Adams DJ Controlled Release from Modified Amino Acid Hydrogels Governed by Molecular Size or Network Dynamics. Langmuir 2009, 25, 10285–10291. [PubMed: 19499945]
56. Adams DJ; Morris K; Chen L; Serpell LC; Bacsa J; Day GM The delicate balance between gelation and crystallisation: structural and computational investigations. Soft Matter 2010, 6, 4144–4156.

57. Wang J; Liu K; Xing R; Yan X Peptide self-assembly: thermodynamics and kinetics. Chem. Soc. Rev. 2016, 45, 5589–5604. [PubMed: 27487936]
58. Liyanage W; Brennessel WW; Nilsson BL Spontaneous Transition of Self-assembled Hydrogel Fibrils into Crystalline Microtubes Enables a Rational Strategy To Stabilize the Hydrogel State. Langmuir 2015, 31, 9933–9942. [PubMed: 26305488]
59. Yuan C; Ji W; Xing R; Li J; Gazit E; Yan X Hierarchically oriented organization in supramolecular peptide crystals. Nat. Rev. Chem. 2019, 3, 567–588.
60. Houton KA; Morris KL; Chen L; Schmidtmann M; Jones JTA; Serpell LC; Lloyd GO; Adams DJ On Crystal versus Fiber Formation in Dipeptide Hydrogelator Systems. Langmuir 2012, 28, 9797–9806. [PubMed: 22651803]
61. Fichman G; Guterman T; Damron J; Adler-Abramovich L; Schmidt J; Kesselman E; Shimon LJW; Ramamoorthy A; Talmon Y; Gazit E Spontaneous structural transition and crystal formation in minimal supramolecular polymer model. Sci. Adv. 2016, 2, e1500827. [PubMed: 26933679]
62. Barker EC; Martin AD; Garvey CJ; Goh CY; Jones F; Mocerino M; Skelton BW; Ogden MI; Becker T Thermal annealing behaviour and gel to crystal transition of a low molecular weight hydrogelator. Soft Matter 2017, 13, 1006–1011. [PubMed: 28083581]
63. Wang Y; Tang L; Yu J Investigation of Spontaneous Transition from Low-Molecular-Weight Hydrogel into Macroscopic Crystals. Cryst. Growth Des. 2008, 8, 884–889.
64. Ryan DM; Anderson SB; Nilsson BL The influence of side-chain halogenation on the self-assembly and hydrogelation of Fmoc-phenylalanine derivatives. Soft Matter 2010, 6, 3220–3231.
65. Ryan DM; Doran TM; Anderson SB; Nilsson BL Effect of C-Terminal Modification on the Self-Assembly and Hydrogelation of Fluorinated Fmoc-Phe Derivatives. Langmuir 2011, 27, 4029–4039. [PubMed: 21401045]
66. Liyanage W; Nilsson BL Substituent Effects on the Self-Assembly/Coassembly and Hydrogelation of Phenylalanine Derivatives. Langmuir 2016, 32, 787–799. [PubMed: 26717444]
67. Chen L; Morris K; Laybourn A; Elias D; Hicks MR; Rodger A; Serpell L; Adams DJ Self-Assembly Mechanism for a Naphthalene−Dipeptide Leading to Hydrogelation. Langmuir 2010, 26, 5232–5242. [PubMed: 19921840]
68. Nanda J; Biswas A; Banerjee A Single amino acid based thixotropic hydrogel formation and pH-dependent morphological change of gel nanofibers. Soft Matter 2013, 9, 4198–4208.
69. Matsumoto S; Yamaguchi S; Ueno S; Komatsu H; Ikeda M; Ishizuka K; Iko Y; Tabata KV; Aoki H; Ito S; Noji H; Hamachi I Photo Gel–Sol/Sol–Gel Transition and Its Patterning of a Supramolecular Hydrogel as Stimuli-Responsive Biomaterials. Chemistry – A European Journal 2008, 14, 3977–3986.
70. Das D; Maiti S; Brahmachari S; Das PK Refining hydrogelator design: soft materials with improved gelation ability, biocompatibility and matrix for in situ synthesis of specific shaped GNP. Soft Matter 2011, 7, 7291–7303.
71. Shi J; Gao Y; Yang Z; Xu B Exceptionally small supramolecular hydrogelators based on aromatic–aromatic interactions. Beilstein J. Org. Chem. 2011, 7, 167–172. [PubMed: 21448260]
72. Yang Z; Liang G; Ma M; Gao Y; Xu B Conjugates of naphthalene and dipeptides produce molecular hydrogelators with high efficiency of hydrogelation and superhelical nanofibers. J. Mater. Chem. 2007, 17, 850–854.
73. Reddy A; Sharma A; Srivastava A Optically Transparent Hydrogels from an Auxin–Amino-Acid Conjugate Super Hydrogelator and its Interactions with an Entrapped Dye. Chemistry – A European Journal 2012, 18, 7575–7581.
74. Raeburn J; Pont G; Chen L; Cesbron Y; Lévy R; Adams DJ Fmoc-diphenylalanine hydrogels: understanding the variability in reported mechanical properties. Soft Matter 2012, 8, 1168–1174.
75. Dawn A; Kumari H Low Molecular Weight Supramolecular Gels Under Shear: Rheology as the Tool for Elucidating Structure–Function Correlation. Chemistry – A European Journal 2017, 24, 762–776.
76. Gupta JK; Adams DJ; Berry NG Will it gel? Successful computational prediction of peptide gelators using physicochemical properties and molecular fingerprints. Chem. Sci. 2016, 7, 4713–4719. [PubMed: 30155120]

77. Frederix PWJM; Scott GG; Abul-Haija YM; Kalafatovic D; Pappas CG; Javid N; Hunt NT; Ulijn RV; Tuttle T Exploring the sequence space for (tri-)peptide self-assembly to design and discover new hydrogels. Nat. Chem. 2014, 7, 30–37. [PubMed: 25515887]

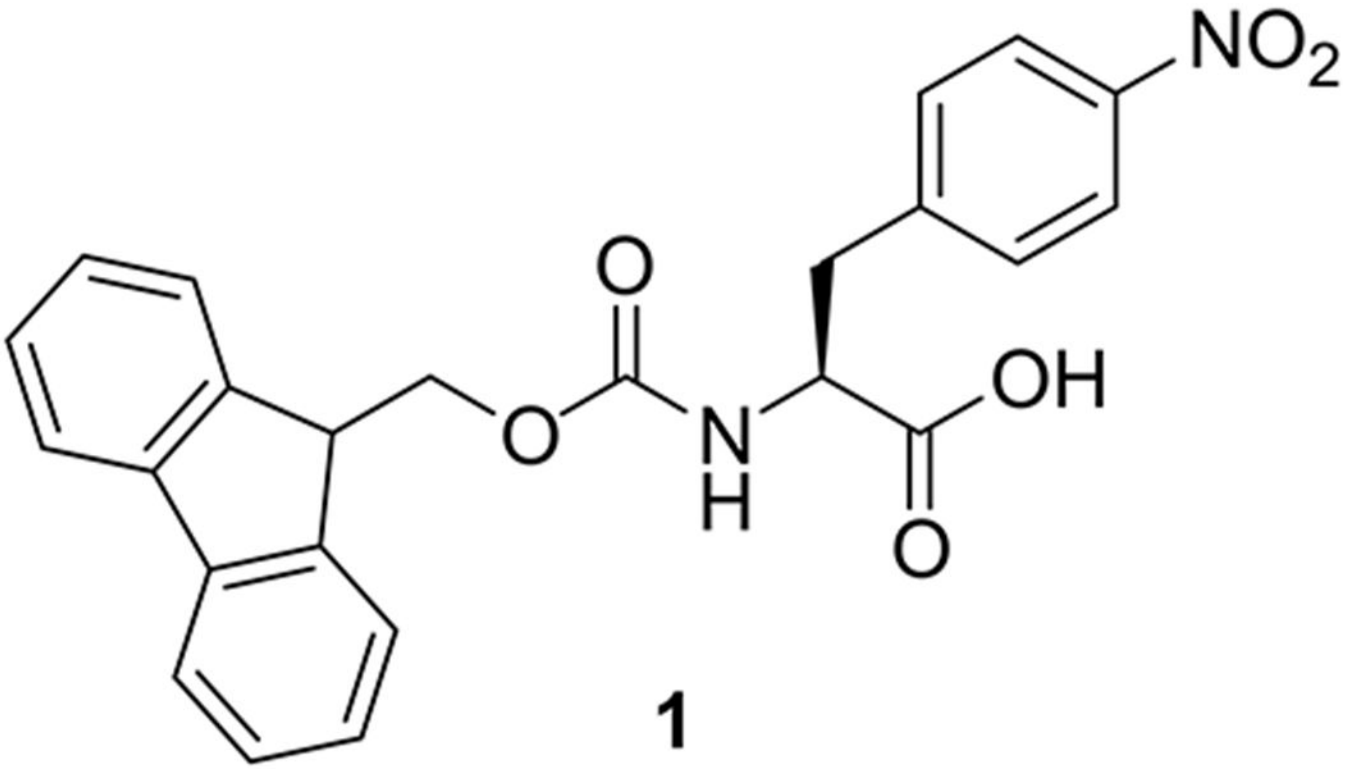

Figure 1.
Chemical structure of Fmoc-4-NO_2-Phe (**1**).

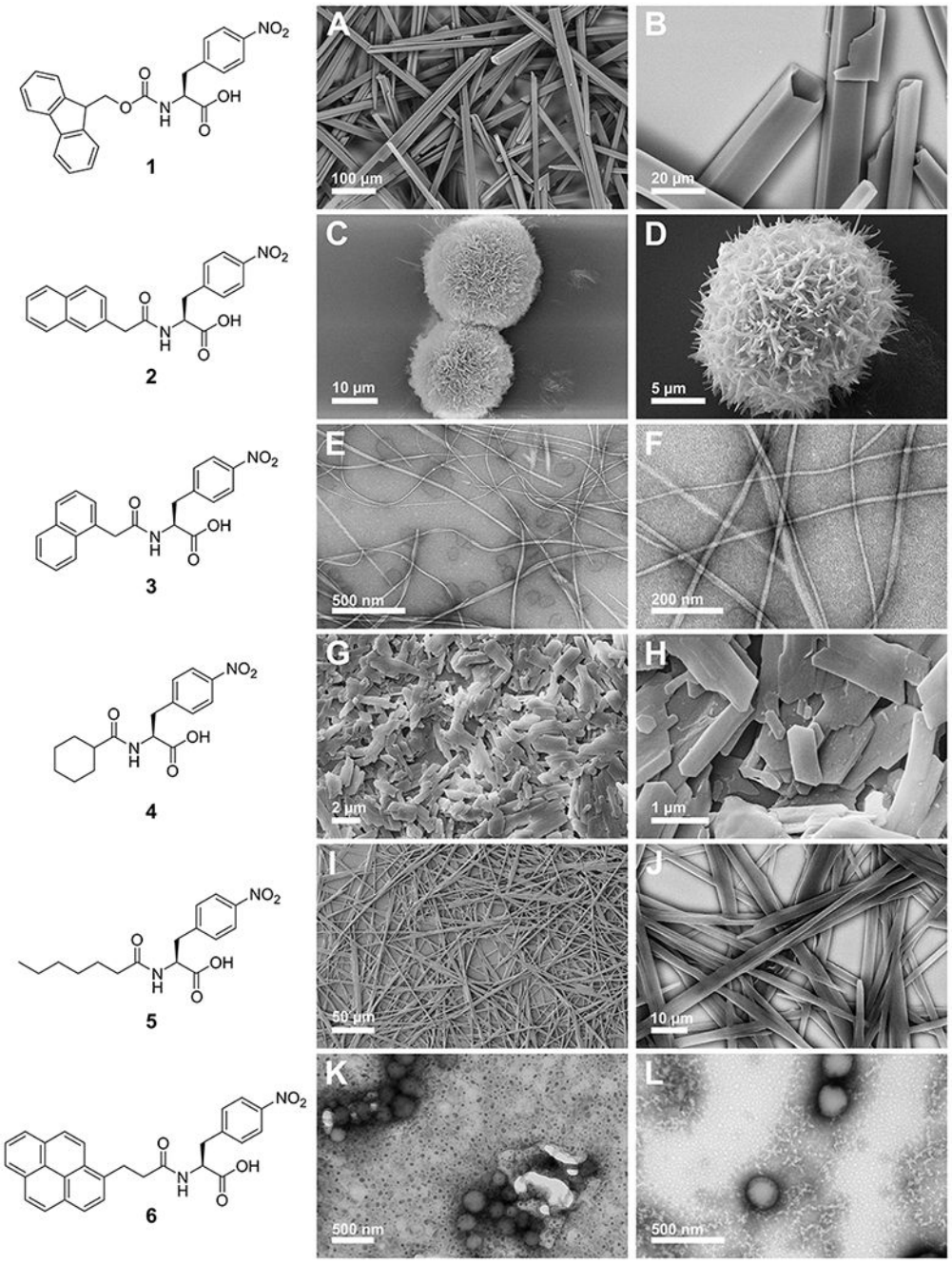

Figure 2.

Representative SEM/TEM images of self-assembled nanostructures formed by compounds **1**-**6**. **A**, **B**. SEM images of crystals of **1**; **C**, **D**. SEM images of crystalline florets of **2**; **E**, **F**. TEM images of fibrils of **3**; **G**, **H**. SEM images of crystals of **4**; **I**, **J**. SEM images of crystal-like assemblies of **5**; **K**, **L**. TEM images of precipitated material of **6**.

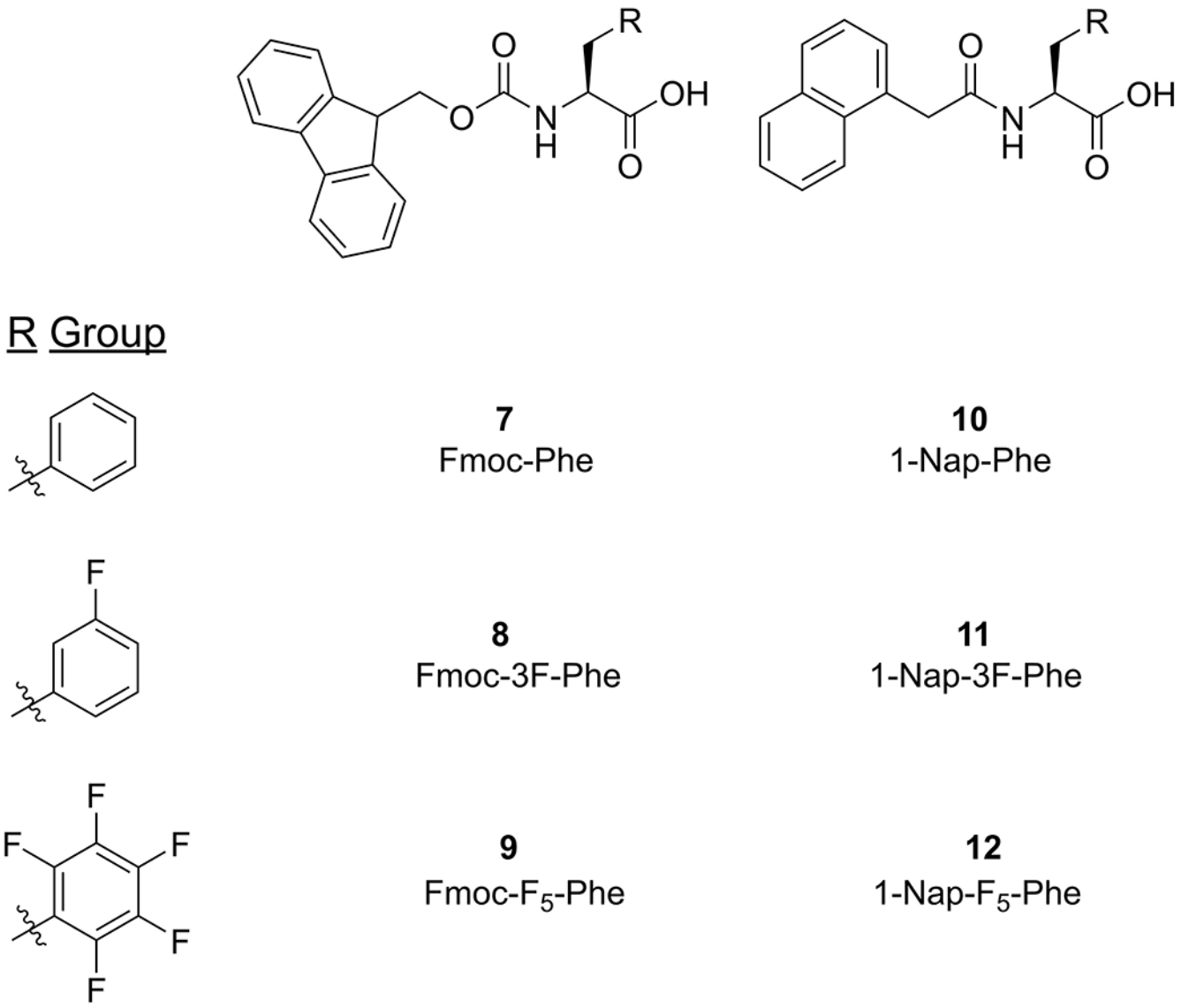

Figure 3.

Chemical structures of Fmoc-Phe derivatives: Fmoc-Phe (**7**), Fmoc-3F-Phe (**8**), Fmoc-F_5-Phe (**9**). Chemical structures of 1-Nap-Phe derivatives: 1-Nap-Phe (**10**), 1-Nap-3F-Phe (**11**), 1-Nap-F_5-Phe (**12**).

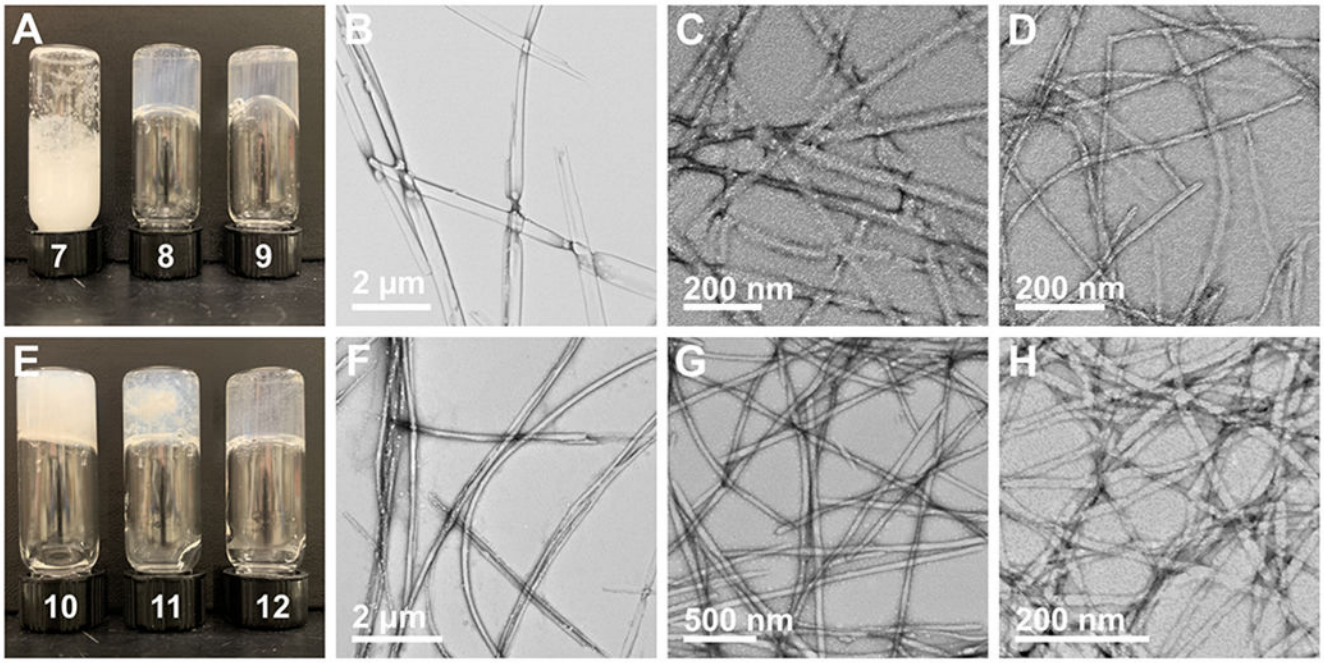

Figure 4.

Digital images and representative TEM images of compounds **7**-**12** self-assembled via the DMSO solvent switch method. (A) Digital image of self-assembled materials of compounds **7**, **8**, and **9** from left to right; (B) TEM image of assembled structures from compound **7**; (C) TEM image of fibrils of compound **8**; (D) TEM image of fibrils of compound **9**; (E) Digital image of self-assembled materials of compounds **10**, **11**, and **12** from left to right; (F) TEM image of fibrils of compound **10**; (G) TEM image of fibrils of compound **11**; (H) TEM image of fibrils of compound **12**.

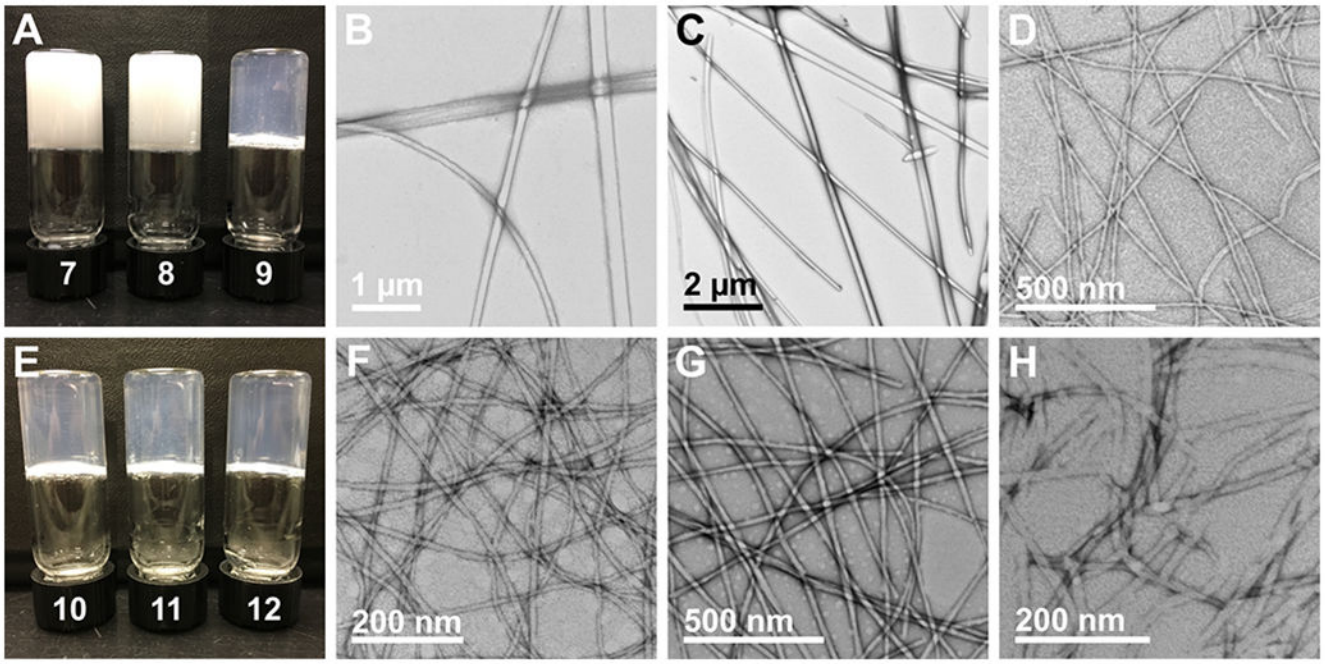

Figure 5.

Digital images and representative TEM images of compounds **7**-**12** self-assembled via the GdL pH switch method. (A) Digital image of self-assembled materials of compounds **7**, **8**, and **9** from left to right; (B) TEM image of assemblies of compound **7**; (C) TEM image of fibrils of compound **8**; (D) TEM image of fibrils of compound **9**; (E) Digital image of self-assembled hydrogels of compounds **10**, **11**, and **12** from left to right; (F) TEM image of fibrils of compound **10**; (G) TEM image of fibrils of compound **11**; (H) TEM image of fibrils of compound **12**.

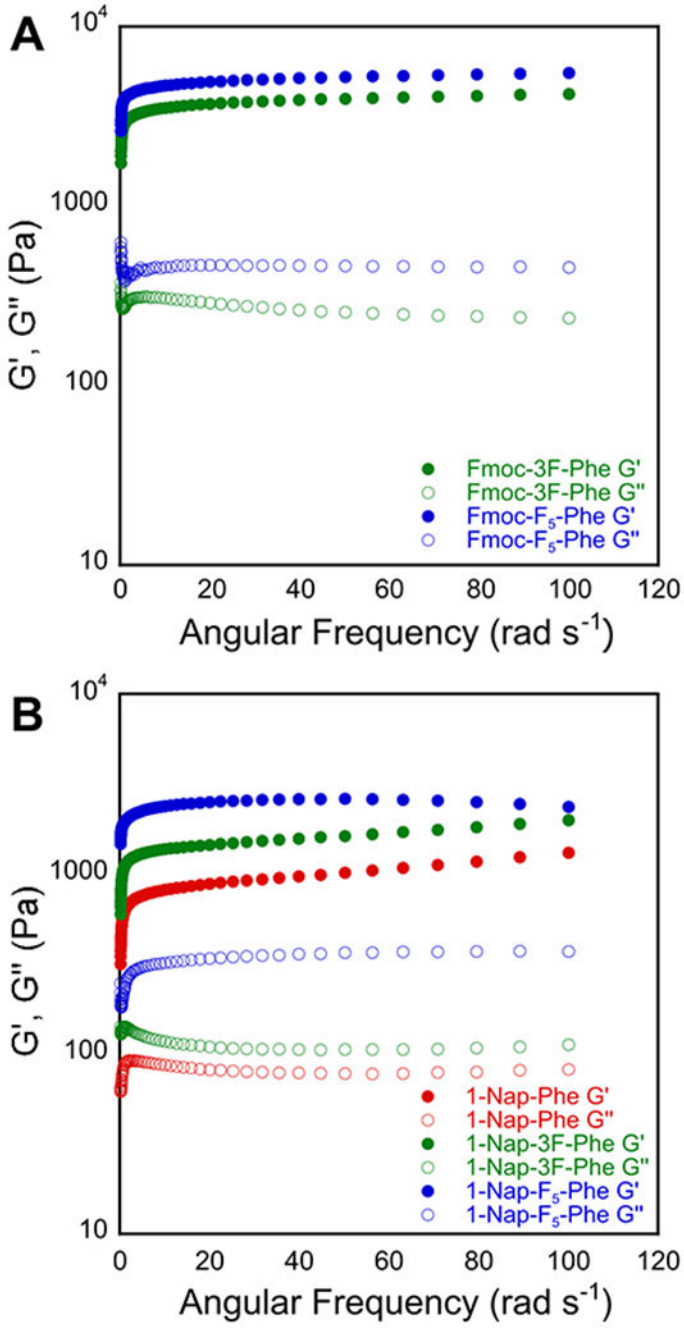

Figure 6.

Representative frequency sweep data collected via oscillatory rheology for compounds **8**-**12**. G′ and G″ values (Pa) are represented by closed circles and open circles, respectively. (A) Frequency sweeps shown for compound **8** in green and compound **9** in blue. (B) Frequency sweeps shown for compound **10** in red, compound **11** in green, and compound **12** in blue.

Table 1.

Rheological properties of hydrogels of compounds **8**-**12** formed by the GdL pH switch method.

Compound	G′ (Pa)	G″ (Pa)
8	3918 ± 338	296 ± 10
9	4786 ± 318	449 ± 17
10	941 ± 8	82 ± 8
11	1548 ± 56	118 ± 6
12	2522 ± 50	336 ± 21